

Light sterile neutrino and leptogenesis

Ki-Young Jung,^a Kim Siyeon^{a,1}

^a*Department of Physics, Chung-Ang University, Seoul 06974 Korea*

E-mail: dmsrl1100@cau.ac.kr, siyeon@cau.ac.kr

ABSTRACT: We studied models of leptogenesis where three right-handed Majorana neutrinos are involved and the minimal-extended seesaw mechanism including an additional singlet field produces four light neutrinos. This study shows that the type of mass ordering and heavy Majorana scales can be determined by inputting the simplest orthogonal matrix into the Casas-Ibarra(CI) representation of seesaw. The CP asymmetry produced from the decays of heavy neutrinos and the dilution mass are predicted in terms of the mass and mixing elements of the fourth neutrino. Upon the choice of CI matrix, the existence of a light sterile neutrino is required to explain the high-energy lepton asymmetry in light of phenomenological measurements. Although there are several free parameters attributable to an additional neutrino, the model can be in part constrained by low-energy experiments such as sterile neutrino searches and neutrinoless double-beta decays, as well as the observed baryon asymmetry in the universe.

KEYWORDS: leptogenesis, sterile neutrino, neutrinoless double-beta decay, minimal extended seesaw

ARXIV EPRINT: [2205.13860](https://arxiv.org/abs/2205.13860)

¹Corresponding author.

Contents

1	Introduction	1
2	Low-energy constraints: CP violation and Lepton number violation	3
3	Extended seesaw mechanism	5
3.1	Simple choices for CI matrix with three right-hand neutrinos	5
3.2	Minimal extended seesaw mechanism	7
4	Leptogenesis from heavy Majorana neturino decays	9
5	light sterile neutrino as probe of leptogenesis	12
5.1	m_{ee}	12
5.2	Y_B vs m_{ee}	14
6	Concluding remarks	14
A	4×4 unitary transformation	15

1 Introduction

Neutrino Physics is about to turn the corner on its way. Next-generation neutrino oscillation experiments under construction, such as DUNE[1] and HK[2], will measure the ordering of masses and CP violation phase in Potecorvo-Maki-Nakagawa-Sakata(PMNS) matrix [3][4] to complete a puzzle board of three massive neutrinos. In addition to mass, mixing angles, and CP violations in the three-neutrino frame, there are other fundamental problems and efforts have been made to address those problems [5]. For example, to understand whether a neutrino is a Majorana particle, a number of neutrinoless double beta decay experiments [6–14] are being conducted, and next-generation experiments such as Legend[15], KamLAND2-Zen[16], and AMoRE-II[17] that can determine the effective mass of electron neutrino m_{ee} with aggressive sensitivity will also be launched. Another issue is the mass-induced oscillations between active neutrinos and sterile neutrino. Short-baseline oscillation experiments using electron antineutrinos from reactors[18–24] and those using muon neutrinos(antineutrinos) from accelerator-based beam lines[25, 26] were performed to find the mixing angles and mass of the fourth neutrino. Assuming that the mass of the fourth neutrino is on the order of 1 eV, more precise experiments such as SBN[27] and JSNS²[28] are underway to obtain data in the near future.

Lepton number violation is generated from processes including Majorana neutrino. Majorana neutrinos that existed with masses near GUT scale in early universe could produce

lepton asymmetry before sphaleron process at electroweak scale [29]. Thus the baryogenesis via leptogenesis[30][31] is one of the natural explanation for the observed baryon asymmetry[32]. As in Sakharov's three conditions for matter-antimatter asymmetry [33], the generation of lepton asymmetry also requires sufficient CP violation in lepton decay, and a careful balance of the produced asymmetry and washout effect, which is done by comparing the decay width to the Hubble expansion rate [34]. The CP-violating decay of a Majorana neutrino via Yukawa coupling requires the vertex contribution of one-loop level including different neutrinos[35–37]. At least two right-hand(RH) neutrinos are needed for Yukawa matrix to contain a phase, and so the leptogenesis with two heavy neutrinos is called the minimal model [38, 39]. It is minimal also in a sense that the lepton asymmetry is described mostly in terms of measurable quantities at low energy. Previous works on minimal models [40, 41] motivated a model extension to three heavy neutrinos without approximation. If all scales of RH neutrinos of seesaw mechanism are higher than 10^{12} GeV, lepton flavor contribution in the decays of heavy neutrinos is excluded out of consideration for the leptogenesis [42–44]. The scales of three heavy neutrinos are assumed to be hierarchically different so that the resonance from the self-energy contribution is avoided [45].

Seesaw mechanism that connects low-energy sector to GUT-scale enables to furnish Yukawa matrix in terms of light masses, low-energy transformation elements, and furthermore heavy Majorana neutrinos. Canonical seesaw mechanism gives rise to three light masses by leveraging three active neutrinos up with two or three heavy ones. According to Casas-Ibarra(CI) expression, the complexity of a 3-by-3 Yukawa matrix cannot be generated unless the CI orthogonal matrix contains complex angles [46]. Models in this article include only real CI rotations for seesaw mechanism, and construct so-called extended Dirac matrix, a 4-by-3 matrix consisting of a 3-by-3 Dirac matrix and 1-by-3 Majorana matrix. In minimal extended seesaw(MES) model, additional Majorana mass terms are originated by the coupling of heavy Majorana neutrino with a lighter Majorana neutrino. If the additional masses are comparable to Dirac masses, they can be a part of the extended Dirac matrix and get involved in seesaw mechanism [47–51]. In this study, the complex Yukawa couplings are traced from a non-unitary partial block of the unitary 4-neutrino mixing matrix, unlike other approaches where the necessary complexity were traced from complex CI angles.

Currently available phenomenological constraints are (i) observed matter-antimatter asymmetry Y_B [32], (ii) effective electron-neutrino masses m_{ee} in neutrinoless double-beta decays[52], and (iii) the elements of PMNS matrix and extended mixing elements with fourth neutrino from oscillation experiments[53][54]. Both normal ordering(NO) and inverted ordering(IO) are yet candidates of mass ordering, while the Dirac phase in PMNS excluded zero from its range at 3σ CL [55][56]. Including one sterile neutrino to the light Majorana neutrino content doubles the number of mixing angles and the number of phases, respectively. It is difficult to test the accessibility of phenomenological observations because phases are added that are either too many or too complicate to measure with known methods. In the near future, we should explore the possibility to ruling out, at least in part, the domains of parameters through experiments that may yield new results one by one.

The outline of contents is as follows: Section II describes the current status of the phenomenology of Majorana neutrinos. Section III introduces a seesaw mechanism model for three neutrinos and MES for four neutrinos. The choice of CI orthogonal matrix determines whether the model is NO or IO. Section IV validates that the model-generated lepton asymmetry is consistent with the observation of baryon asymmetry, and identifies the correlations between different mass scales. In Section V, different phenomena m_{ee} and Y_B are estimated simultaneously in terms of combinations of phases, both Dirac and Majorana. Contours of m_{ee} and Y_B are drawn for the possibility that the ranges of those phases can be excluded in future experiments. It is followed by concluding remarks.

2 Low-energy constraints: CP violation and Lepton number violation

Three neutrinos that couple with weak bosons in the Standard Model(SM) are mixed states of the neutrinos defined by their masses. The unitary PMNS mixing matrix V for 3 generations of neutrinos is given by

$$V = R(\theta_{23}) R(\theta_{13}, \delta) R(\theta_{12}) \quad (2.1)$$

where each R is a rotation matrix with a mixing angle θ_{ij} between i -th and j -th generations. According to the standard parametrization, the Dirac phase δ is combined with the smallest angle θ_{13} as in $\sin \theta_{13} e^{-i\delta}$ in the PMNS matrix. The detailed matrix form in terms of three angles and a phase is given in Eq.(A.1). Under assumption that neutrinos are Majorana particles, a diagonal phase transformation P_2 in Eq.(A.2) is attached to V such that the Majorana phases η_1 and η_2 can be a part of the mass matrix of light neutrinos in the following way:

$$M_\nu = V^* \text{Diag}(\tilde{m}_1, \tilde{m}_2, m_3) V^\dagger, \quad (2.2)$$

where $\tilde{m}_1 \equiv m_1 e^{-2i\eta_1}$ and $\tilde{m}_2 \equiv m_2 e^{-2i\eta_2}$. The notations and conventions for masses and transformation matrices in this work are taken from PDG [57]. The PMNS matrix is then expressed as $U \equiv V P_2$.

Neutrinoless double-beta decay $0\nu\beta\beta$ is a known process as related to all phases in U and its half life is given by

$$\left(T_{1/2}^{0\nu}\right)^{-1} = G_{0\nu} |\mathcal{M}_{0\nu}|^2 m_{ee}^2, \quad (2.3)$$

where $G_{0\nu}$ and $\mathcal{M}_{0\nu}$ are the phase space factor and the nuclear matrix element of the $0\nu\beta\beta$, respectively. The decay rate of normal double-beta decay is simply given by $G_{0\nu} |\mathcal{M}_{0\nu}|^2$ without m_{ee} . The effective Majorana mass of electron neutrino mass m_{ee} is the only neutrino-dependent factor in the decay width, which is given as

$$m_{ee} \equiv |\tilde{m}_1 U_{e1}^2 + \tilde{m}_2 U_{e2}^2 + m_3 U_{e3}^2|. \quad (2.4)$$

It can be expressed more explicitly in terms of phases as

$$\begin{aligned} m_{ee}^2 = & m_1^2 |U_{e1}|^4 + m_2^2 |U_{e2}|^4 + m_3^2 |U_{e3}|^4 \\ & + 2m_1 m_2 \cos 2(\eta_2 - \eta_1) |U_{e1}|^2 |U_{e2}|^2 \\ & + 2m_1 m_3 \cos 2(\eta_1 + \delta) |U_{e1}|^2 |U_{e3}|^2 \\ & + 2m_2 m_3 \cos 2(\eta_2 + \delta) |U_{e2}|^2 |U_{e3}|^2. \end{aligned} \quad (2.5)$$

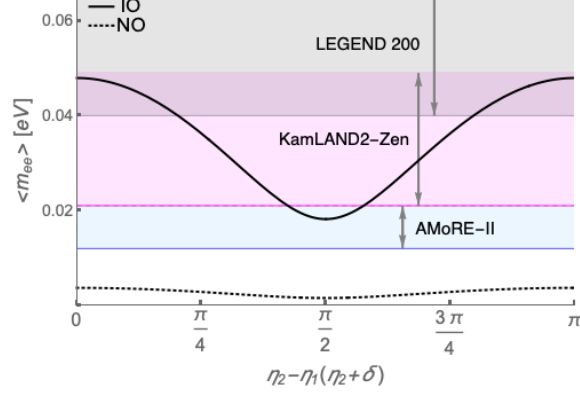


Figure 1. m_{ee} vs. phases. If mass ordering is hierarchical, the phase dependency is monotonous. In the effective Majorana mass, $\cos 2(\eta_2 + \delta)$ term is dominant for NO, while $\cos 2(\eta_2 - \eta_1)$ is dominant for IO. The 3σ sensitivities of m_{ee} that future experiments aim for are known as 40-73 meV for LEGEND200, 21-49 meV for KamLAND2-Zen, and 12-21 meV for AMoRE-II.

The current values of neutrino masses and mixing angles and CP phase based on various oscillation experiments are as follows [57][58][59]:

$$\begin{aligned} \Delta m_{21}^2 &= (7.53 \pm 0.18) \times 10^{-5} \text{ (eV)}^2 & \text{NO} \\ \sin^2 \theta_{12} &= (0.307 \pm 0.013) & \text{IO} \\ \sin^2 \theta_{13} &= (2.20 \pm 0.07) \times 10^{-2} \end{aligned} \quad (2.6)$$

$$\begin{aligned} \Delta m_{32}^2 &= (2.453 \pm 0.033) \times 10^{-3} \text{ (eV)}^2 & \text{NO} \\ \sin^2 \theta_{23} &= (0.546 \pm 0.021) \end{aligned} \quad (2.7)$$

$$\begin{aligned} \Delta m_{32}^2 &= (-2.536 \pm 0.034) \times 10^{-3} \text{ (eV)}^2 & \text{IO} \\ \sin^2 \theta_{23} &= (0.539 \pm 0.022) \end{aligned} \quad (2.8)$$

$$\begin{aligned} \delta/\pi &= 1.08 + 0.13(-0.12) & \text{NO} \\ \delta/\pi &= 1.58 + 0.15(-0.16) & \text{IO} \end{aligned} \quad (2.9)$$

where NO means $m_1 < m_2 < m_3$ order and IO means $m_3 < m_2 < m_1$ order. Referring Eq.(2.5), for NO, m_{ee} obtains the maximum with $\eta_2 + \delta = 0$ or π and the minimum with $\eta_2 + \delta = \pi/2$. For IO, the maximum m_{ee} comes up with $\eta_2 - \eta_1 = 0$ or π and the minimum with $\pi/2$. The curves in Fig.1 show the aspect straightforward. As upcoming $0\nu\beta\beta$ search experiments improve the sensitivity of m_{ee} , they can first test mass type IO and can rule out some range of $\eta_2 - \eta_1$. As can be seen from the figure, the sensitivities of the known experiments do not approach to that of NO type, although NO is somehow favored by oscillation experiments [55][56]. If the neutrino mass type is NO and $0\nu\beta\beta$ is found in the experiments with sensitivity in the range 10 - 60 meV, it is necessary to modify the neutrino mass structure.

3 Extended seesaw mechanism

3.1 Simple choices for CI matrix with three right-hand neutrinos

Canonical model of seesaw mechanism to suppress neutrino masses below 1 eV using heavy neutrino mass scale requires $SU(2)$ Higgs doublet, whose existence was experimentally confirmed [60][61]. To the following SM contents:

- left-hand lepton doublets $L_\ell = (\nu_\ell \ell_L)_i^T$,
- right-hand lepton singlets ℓ_R ,
- Higgs doublet $H = (\phi^+ \phi^0)^T$,

where ℓ is the index for e, μ , and τ , non-SM singlet neutrinos N_R 's are added to give rise to Yukawa couplings to neutrinos, and the Majorana mass term of N_R is accordingly constructed. After spontaneous symmetry breaking of $SU(2)$ by the vacuum expectation value $\langle \phi^0 \rangle = v$, the lepton mass terms of lagrangian reduces to

$$-\mathcal{L}_{\text{mass}} = v\mathcal{Y}_\ell \bar{\ell}_L \ell_R + v\mathcal{Y}_\nu \bar{\nu}_\ell N_R^c + \frac{1}{2}M_R \bar{N}_R N_R^c + \text{h.c.}, \quad (3.1)$$

with $v = 246/\sqrt{2}$ GeV. In terms of flavors, we consider 3-generation Majorana neutrinos motivated from $SO(10)$ grand unified theory. The model is constructed on the basis where heavy Majorana neutrinos and charged leptons are represented by $N_R = (N_1 \ N_2 \ N_3)^T$ and $\ell_L = (e_L \ \mu_L \ \tau_L)^T$ and their masses M_R and \mathcal{Y}_ℓ are diagonal. The 3×3 neutrino Yukawa matrix \mathcal{Y}_ν alone is non-diagonal on the basis of $\nu_\ell = (\nu_e \ \nu_\mu \ \nu_\tau)^T$ which are the weak interaction partners of the charged leptons ℓ_L . It is possible to express the neutrino mass term in Eq.(3.1) on $(\nu_\ell^T \ (N_R^c)^T) = (\nu_e \ \nu_\mu \ \nu_\tau \ N_1^c \ N_2^c \ N_3^c)$ such as

$$-\mathcal{L}_{\text{nu-mass}} = \begin{pmatrix} \bar{\nu}_\ell & \bar{N}_R \end{pmatrix} \begin{pmatrix} 0 & v\mathcal{Y}_\nu \\ v\mathcal{Y}_\nu^T & M_R \end{pmatrix} \begin{pmatrix} \nu_\ell \\ N_R^c \end{pmatrix}, \quad (3.2)$$

where \mathcal{Y}_ν and M_R are 3×3 matrices. The seesaw mechanism is a block diagonalization to separate the mass matrices of light neutrinos from heavy ones. The light Majorana masses is lifted by stepping on heavy Majorana neutrinos such as

$$M_\nu = -v^2 \mathcal{Y}_\nu M_R^{-1} \mathcal{Y}_\nu^T, \quad (3.3)$$

which is equivalent to the mass matrix in Eq.(2.2).

Casas-Ibarra parametrization rephrases the seesaw mechanism to find the Dirac mass matrix $v\mathcal{Y}_\nu$ in terms of light Majorana masses and heavy Majorana masses such as [46],

$$v\mathcal{Y}_\nu = U^* \sqrt{m_L} \mathcal{O} \sqrt{M_R}, \quad (3.4)$$

where both m_L and M_R represent the diagonal mass matrices for light neutrinos and heavy neutrinos, respectively. The transformation matrix U corresponds to the PMNS matrix. The orthogonal matrix \mathcal{O} on the right-hand side is the only input that can control the structure of Yukawa matrix. In other words, a model of Yukawa matrix can be generated by the

choice of an orthogonal matrix \mathcal{O} in Eq.(3.4). Three dimensional orthogonal transformation is parametrized by three rotations, $R(\varrho_{13})$, $R(\varrho_{23})$, and $R(\varrho_{12})$, which were assumed to be complex in Ref.[46]. In this study, special choices of real angles are attempted. For example, the choice A is named for the following Dirac matrix

$$v\mathcal{Y}_A = vU^*\mathcal{O}_A \quad (3.5)$$

with

$$\mathcal{O}_A = \begin{pmatrix} 0 & 0 & 1 \\ 0 & 1 & 0 \\ -1 & 0 & 0 \end{pmatrix} \quad (3.6)$$

obtained with $\varrho_{12} = \varrho_{23} = 0$, and $\varrho_{13} = \pi/2$. If that simple choice is made for Dirac matrix, the seesaw mechanism in Eq.(3.3) reduces to the following relation

$$(m_1, m_2, m_3)_A = v^2 \left(\frac{1}{M_3}, \frac{1}{M_2}, \frac{1}{M_1} \right), \quad (3.7)$$

and the Yukawa matrix is expressed in terms of only neutrino mixing matrix U such as $\mathcal{Y}_A = (-U_{\alpha 3}^* \ e^{-i\eta_2} U_{\alpha 2}^* \ e^{-i\eta_1} U_{\alpha 1}^*)$ with $U_{\alpha i} = (U_{ei} \ U_{\mu i} \ U_{\tau i})^T$. The above model explains that the NO mass $m_1 < m_2 < m_3$ is the consequence of a simple choice of \mathcal{O}_A and $\mathcal{Y}_A = U^*\mathcal{O}_A$. For NO, whether the mass squared differences of Eq.(2.6) and Eq.(2.7) are hierarchical or quasi-degenerate, the type of difference remains open. The numerical values of light masses from Eq.(2.6) and Eq.(2.7) are $(m_2, m_3) = (8.68 \times 10^{-3}, 4.95 \times 10^{-2})$ eV, and the bottom-up estimation of heavy masses is $(M_1, M_2) = (6.06 \times 10^{14}, 3.78 \times 10^{15})$ GeV. The mass scale M_3 is much higher than M_2 so that m_1 can be considered close to zero.

Another choice is constructed from the following Dirac matrix,

$$v\mathcal{Y}_B = vU^*\mathcal{O}_B \quad (3.8)$$

with

$$\mathcal{O}_B = \begin{pmatrix} 0 & 1 & 0 \\ -1 & 0 & 0 \\ 0 & 0 & 1 \end{pmatrix}, \quad (3.9)$$

which is an orthogonal matrix with $\varrho_{13} = \varrho_{23} = 0$, and $\varrho_{12} = \pi/2$. If Yukawa matrix is chosen as $\mathcal{Y}_B = U^*\mathcal{O}_B$ so that $\mathcal{Y}_B = (-e^{-i\eta_2} U_{\alpha 2}^* \ e^{-i\eta_1} U_{\alpha 1}^* \ U_{\alpha 3}^*)$ with $U_{\alpha i} = (U_{ei} \ U_{\mu i} \ U_{\tau i})^T$, the masses of light neutrinos are determined by the heavy masses in another simple way,

$$(m_1, m_2, m_3)_B = v^2 \left(\frac{1}{M_2}, \frac{1}{M_1}, \frac{1}{M_3} \right), \quad (3.10)$$

which describes the inverted ordering(IO) $m_3 < m_1 < m_2$ from the heavy Majorana mass order $M_1 < M_2 < M_3$. It is worth paying attention to the mass relations in Eq.(3.10) that implies the quasi-degeneracy in Majorana mass scales M_1 and M_2 . In IO, the m_1 and m_2 are constrained in the same order of magnitude, because m_2 is bounded by $\Delta m_{32}^2 =$

$(-2.54 \pm 0.03) \times 10^{-3} \text{eV}^2$, whereas m_1 is limited by $\Delta m_{21}^2 = (7.53 \pm 0.18) \times 10^{-5} \text{eV}^2$. The quasi-degeneracy in the above IO choice appears in the relation between M_1 and M_2 . The numerical values from the best-fit in Eq.(2.6) and Eq.(2.8) are $(m_1, m_2) = (4.96 \times 10^{-2}, 5.04 \times 10^{-2}) \text{eV}$ and the heavy masses are $(M_1, M_2) = (6.01 \times 10^{14}, 6.10 \times 10^{14}) \text{GeV}$. The mass scale M_3 is much higher than M_2 so that m_3 can be considered close to zero. The generalization of \mathcal{O} with ϱ_{ij} s that are deviated from 0 or $\pi/2$ is also under study.

3.2 Minimal extended seesaw mechanism

An additional singlet neutrino S is introduced such that the Lagrangian in Eq.(3.1) is modified to

$$-\mathcal{L}_{\text{mass}} + M_S \bar{S}^c N_R + \text{h.c.}, \quad (3.11)$$

resulting in another Majorana mass M_S . Then the full contribution for neutrino masses is constructed on the basis $(\nu_\ell^T (N_R^c)^T S^c) = (\nu_e \nu_\mu \nu_\tau N_1^c N_2^c N_3^c S^c)$,

$$-\mathcal{L}_{\text{MES}} = \begin{pmatrix} \bar{\nu}_\ell & \bar{N}_R & \bar{S} \end{pmatrix} \begin{pmatrix} 0 & v\mathcal{Y}_\nu & 0 \\ v\mathcal{Y}_\nu^T & M_R & M_S^T \\ 0 & M_S & 0 \end{pmatrix} \begin{pmatrix} \nu_\ell \\ N_R^c \\ S^c \end{pmatrix}, \quad (3.12)$$

assuming that $M_S, M_D \ll M_R$. The scale of 1×3 matrix M_S could be smaller or larger than that of M_D . It is not necessary to place restrictions on the individual elements of M_S and M_D for the condition that the fourth mass must be greater than the other three, as far as the low-energy phenomenological constraints are fulfilled. Taking the seesaw mechanism with respect to the heavy M_R makes it possible to construct the effective mass terms on the light neutrinos $(\nu_\ell^T S^c) = (\nu_e \nu_\mu \nu_\tau S^c)$,

$$M_\nu = - \begin{pmatrix} v\mathcal{Y}_\nu \\ M_S \end{pmatrix} M_R^{-1} \begin{pmatrix} v\mathcal{Y}_\nu^T & M_S^T \end{pmatrix} \quad (3.13)$$

$$= \begin{pmatrix} -v^2 \mathcal{Y}_\nu M_R^{-1} \mathcal{Y}_\nu^T & -v \mathcal{Y}_\nu M_R^{-1} M_S^T \\ -v M_S M_R^{-1} \mathcal{Y}_\nu^T & -M_S M_R^{-1} M_S^T \end{pmatrix} \quad (3.14)$$

which represents the 4×4 matrix of 3 active neutrinos and 1 sterile neutrino. In MES model, the M_S may bring up an eV-order mass for S field via another seesaw $-M_S M_R^{-1} M_S^T$. It is worthwhile stressing that the determinant of M_ν vanishes, indicating that the lightest neutrino is massless [49][50]. The above mass matrix is diagonalized by $U' = U_F' P_3$ in Eq.(A.4) and Eq.(A.7) as follows;

$$m_L' \equiv \text{Diag}(m_1, m_2, m_3, m_4) = U'^T M_\nu U'. \quad (3.15)$$

Casas-Ibarra parametrization for the minimal extended seesaw mechanism can be expressed by

$$\begin{pmatrix} v\mathcal{Y}_\nu \\ M_S \end{pmatrix} = \mathcal{R} U'^* \sqrt{m_L'} \mathcal{O}' \sqrt{M_R}, \quad (3.16)$$

which will be called extended Dirac matrix hereafter. The $\mathcal{R} \equiv \text{Diag}(1, 1, 1, r)$ is placed due to the different origins of $v\mathcal{Y}_\nu$ and M_S . The diagonal $\sqrt{m_L'}$ is now a 4×4 and \mathcal{O}' is a 4×3 matrix that satisfies $\mathcal{O}'^T \mathcal{O}' = \mathbb{I}_{3 \times 3}$. On the other hand, $\mathcal{O}' \mathcal{O}'^T \neq \mathbb{I}_{4 \times 4}$ and so \mathcal{O}' is no longer orthogonal. Similar non-orthogonal matrices were adopted in minimal seesaw model with two right-hand neutrinos for building a 3×2 Dirac matrix [38]. A choice A' is introduced by the following extended Dirac matrix:

$$\begin{pmatrix} v\mathcal{Y}'_A \\ M_S \end{pmatrix} = v\mathcal{R}U'^* \mathcal{O}'_A \quad (3.17)$$

with

$$\mathcal{O}'_A = \begin{pmatrix} 0 & 0 & 0 \\ 0 & 0 & 1 \\ 0 & 1 & 0 \\ -1 & 0 & 0 \end{pmatrix}. \quad (3.18)$$

The masses of light neutrinos are determined by substituting the extended Dirac matrix, $\mathcal{Y}'_A = (-U'^*_{\alpha 4} \ e^{-i\eta_3} U'^*_{\alpha 3} \ e^{-i\eta_2} U'^*_{\alpha 2})$ and $M_S/v = r(-U'^*_{s4} \ e^{-i\eta_3} U'^*_{s3} \ e^{-i\eta_2} U'^*_{s2})$ with $U_{\alpha i} = (U_{ei} \ U_{\mu i} \ U_{\tau i})^T$, into MES in Eq.(3.13)

$$(m_1, m_2, m_3, m_4)'_A = v^2 \left(0, \frac{1}{M_3}, \frac{1}{M_2}, \frac{r^2}{M_1} \right), \quad (3.19)$$

which describes the NO-type light masses $m_2 < m_3 < m_4$ from the heavy Majorana masses $M_1 < M_2 < M_3$. Due to \mathcal{O}'_A , m_1 became the zeroed mass dictated by the vanishing determinant of M_ν in Eq.(3.13). The numerical values from the best-fit are $(m_2, m_3) = (8.68 \times 10^{-3}, 4.95 \times 10^{-2})$ eV and the heavy neutrino scales are $(M_2, M_3) = (6.06 \times 10^{14}, 3.78 \times 10^{15})$ GeV. The mass of the sterile neutrino m_4 can have an eV order with a choice of r and M_1 .

Another choice for the extended Dirac matrix in Eq.(3.16) is

$$\begin{pmatrix} v\mathcal{Y}'_B \\ M_S \end{pmatrix} = v\mathcal{R}U'^* \mathcal{O}'_B \quad (3.20)$$

with

$$\mathcal{O}'_B = \begin{pmatrix} 0 & 0 & 1 \\ 0 & 1 & 0 \\ 0 & 0 & 0 \\ -1 & 0 & 0 \end{pmatrix}. \quad (3.21)$$

Then the IO-type masses of light neutrinos are determined by substituting the extended Dirac matrix, $\mathcal{Y}'_B = (-U'^*_{\alpha 4} \ e^{-i\eta_2} U'^*_{\alpha 2} \ e^{-i\eta_1} U'^*_{\alpha 1})$ and $M_S/v = r(-U'^*_{s4} \ e^{-i\eta_2} U'^*_{s2} \ e^{-i\eta_1} U'^*_{s1})$ with $U_{\alpha i} = (U_{ei} \ U_{\mu i} \ U_{\tau i})^T$, into MES in Eq.(3.13)

$$(m_1, m_2, m_3, m_4)'_B = v^2 \left(\frac{1}{M_3}, \frac{1}{M_2}, 0, \frac{r^2}{M_1} \right), \quad (3.22)$$

where the m_3 is specifically zeroed one due to \mathcal{O}'_B . Like the choice B in Eq.(3.10), the measured mass-squared differences in Eq.(2.8) require a very narrow gap between M_2 and M_3 , which are 6.01×10^{14} GeV and 6.10×10^{14} GeV, respectively.

The r in Eq.(3.16) may be either smaller or larger than one, but it has a lower bound constrained by m_4 and M_1 and an upper bound constrained by M_2 . It has been shown, in Eq.(3.19) and Eq.(3.22), that overall order of the matrix M_S does not need to be larger than the order of M_D to have the m_4 larger than the other three masses.

The best fits and the 3σ ranges of $|U_{e4}|^2$, $|U_{\mu 4}|^2$, $|U_{\tau 4}|^2$ and Δm_{41}^2 are listed in the reference [54] as follows;

	best fit	3σ CL	
$ U_{e4} ^2$	0.0020	$0.0098 \sim 0.031$	(3.23)
$ U_{\mu 4} ^2$	0.0015	$0.0060 \sim 0.026$	
$ U_{\tau 4} ^2$	0.0032	$0.0 \sim 0.039$	
Δm_{41}^2	1.7 eV^2		

where the Δm_{41}^2 available in 3σ CL is not considered in this work because three separate islands of ranges exist yet in the analysis. The elements of M_S are determined by the above experimental values using the relations in Eq.(A.8).

4 Leptogenesis from heavy Majorana neturino decays

A heavy Majorana neutrino N_i decays via Yukawa coupling, and its decay rate at tree level is

$$\begin{aligned}\Gamma_{N_i} &= \Gamma(N_i \rightarrow \ell H) + \Gamma(N_i \rightarrow \bar{\ell} H^*) \\ &= \frac{(\mathcal{Y}_\nu^\dagger \mathcal{Y}_\nu)_{ii} M_i}{8\pi},\end{aligned}\tag{4.1}$$

where M_i is the mass of N_i and \mathcal{Y}_ν is the Yukawa matrix. From the interference between tree-level and one-loop level amplitudes, the CP asymmetry is estimated as

$$\epsilon_i = \frac{\Gamma(N_i \rightarrow \ell H) - \Gamma(N_i \rightarrow \bar{\ell} H^*)}{\Gamma(N_i \rightarrow \ell H) + \Gamma(N_i \rightarrow \bar{\ell} H^*)}\tag{4.2}$$

$$= \frac{\sum_{j \neq i} \text{Im}[(\mathcal{Y}_\nu^\dagger \mathcal{Y}_\nu)_{ji}^2]}{8\pi(\mathcal{Y}_\nu^\dagger \mathcal{Y}_\nu)_{ii}} \left\{ f\left(\frac{M_j^2}{M_i^2}\right) + g\left(\frac{M_j^2}{M_i^2}\right) \right\}\tag{4.3}$$

where $f(x) = \sqrt{x}[1 - (1+x)\ln(\frac{1+x}{x})]$ and $g(x) = \frac{\sqrt{x}}{1-x}$ indicate the contributions from the vertex correction and the self-energy correction, respectively [35][36]. If the difference between M_i and M_j is hierarchical, the self-energy part can be neglected. Though it can become dominant in case of $M_i \sim M_j$, it is out of consideration in this work. The Yukawa coupling of a Majorana neutrino itself violates the lepton number at Lagrangian level, and $\Delta L = 1$ scattering of a Majorana neutrino and $\Delta L = 2$ scattering, $HH \rightarrow \ell\ell$, mediated by a Majorana neutrino are also the sources of lepton number violation.

The survival of the asymmetry from thermal washout effect is estimated from the comparison of the decay rate with the Hubble expansion rate of the Universe at temperature T ,

$$H(T) = \sqrt{\frac{4\pi^3 g_*}{45}} \frac{T^2}{M_{\text{pl}}}, \quad (4.4)$$

where M_{pl} is the Planck scale 1.22×10^{19} GeV and $g_* = 112$ is the degree of freedom of universe with 3 Majorana neutrinos. The ratio of the decay rate to the Hubble parameter at $T = M_1$ is denoted by K_1 , and can be estimated in terms of effective neutrino mass \tilde{m}_1 and equilibrium mass m_* as follows,

$$K_1 \equiv \frac{\Gamma_{N_1}}{H(M_1)} = \frac{\tilde{m}_1}{m_*}, \quad (4.5)$$

where

$$\begin{aligned} \tilde{m}_1 &= \frac{(\mathcal{Y}_\nu^\dagger \mathcal{Y}_\nu)_{11} v^2}{M_1} \\ m_* &= \frac{16\pi^{5/2}}{3\sqrt{5}} \frac{\sqrt{g_*} v^2}{M_{\text{pl}}}. \end{aligned} \quad (4.6)$$

The observed baryon asymmetry normalized over the entropy density is given by $Y_B = (n_B - n_{\bar{B}})/s = (8.61 \pm 0.05) \times 10^{-11}$ [57]. The most well-established theory is that baryon asymmetry was produced from the lepton asymmetry through sphaleron process [34]:

$$Y_B = \frac{a}{a-1} Y_L \quad (4.7)$$

where $a = 28/79$ is determined by $(8N_F + 4N_H)/(22N_F + 13N_H)$ for the Standard Model with the number of fermion generations $N_F = 3$ and a single Higgs doublet $N_H = 1$. The lepton asymmetry Y_L derived from the Yukawa couplings and their interference is expressed by

$$Y_L = \sum_{i=3}^3 \kappa_i \frac{\epsilon_i}{g_*}, \quad (4.8)$$

where the dilution factor κ_i is a function of K . The dilution factor, κ_i , is given by

$$\kappa_i = -\frac{0.3}{K_i (\ln K_i)^{3/5}}, \quad (4.9)$$

in the range $10 \lesssim K_i \lesssim 10^6$ [37][62]. If Majorana neutrinos decay through the Yukawa couplings of choice A in Eq.(3.5) or choice B in Eq.(3.8), the CP asymmetry generated from imaginary parts in off-diagonal elements of $\mathcal{Y}^\dagger \mathcal{Y}$ cannot be produced. The unitarity of U_{PMNS} results in $\mathcal{Y}_A^\dagger \mathcal{Y}_A = \mathbb{I}$ and $\mathcal{Y}_B^\dagger \mathcal{Y}_B = \mathbb{I}$. It is clear that $\text{Im}[(\mathcal{Y}_\nu^\dagger \mathcal{Y}_\nu)_{ji}^2]$ vanishes as long as \mathcal{O} in Eq.(3.4) does not adopt complex angles. Thus, the Davidson-Ibarra bound [63] is not considered since it is built on the base that the CP-violating imaginary part in Yukawa matrix is related with complex angles in the orthogonal matrix \mathcal{O} .

In choice A' in Eq.(3.17) and choice B' in Eq.(3.20), the 3×3 matrices \mathcal{Y}'_A and \mathcal{Y}'_B avoid the unitary property of U'_F and non-vanishing imaginary parts of off-diagonal elements in $\mathcal{Y}'^\dagger \mathcal{Y}'$ give rise to the CP asymmetry ϵ_i . When the mass relations in Eq.(3.19) and Eq.(3.22) are applied, the $\mathcal{Y}'^\dagger \mathcal{Y}'$ are obtained in terms of the elements of mixing matrices including both Dirac and Majorana phases as follows;

$$\mathcal{Y}'^\dagger_A \mathcal{Y}'_A - \mathbb{I} = \begin{pmatrix} |U'_{s4}|^2 & U'^*_{s4} U'_{s3} e^{-i\eta_3} & U'^*_{s4} U'_{s2} e^{-i\eta_2} \\ \checkmark & |U'_{s3}|^2 & -U'^*_{s3} U'_{s2} e^{-i(\eta_2 - \eta_3)} \\ \checkmark & \checkmark & |U'_{s2}|^2 \end{pmatrix}, \quad (4.10)$$

$$\mathcal{Y}'^\dagger_B \mathcal{Y}'_B - \mathbb{I} = \begin{pmatrix} |U'_{s4}|^2 & U'^*_{s4} U'_{s2} e^{-i\eta_2} & U'^*_{s4} U'_{s1} e^{-i\eta_1} \\ \checkmark & |U'_{s2}|^2 & -U'^*_{s2} U'_{s1} e^{-i(\eta_1 - \eta_2)} \\ \checkmark & \checkmark & |U'_{s1}|^2 \end{pmatrix}. \quad (4.11)$$

In each choice, a phase among three Majorana phases in Eq.(A.7) is removed along with a zero mass, and the three Dirac phases introduced in Eq.(A.1) and Eq.(A.5) are imbedded in the elements of U'_F . The elements marked by \checkmark are the complex conjugate of the transposed elements, respectively. The simple choices predict the mass scales of Majorana neutrinos such as

$$\begin{aligned} \text{Choice } A' \text{ and } B' \\ M_1 = r^2 (2.3 \times 10^{13}) \text{ GeV} \end{aligned} \quad (4.12)$$

$$\begin{aligned} \text{Choice } A' \\ M_2 = 6.1 \times 10^{14} \text{ GeV} \\ M_3 = 3.8 \times 10^{15} \text{ GeV} \end{aligned} \quad (4.13)$$

$$\begin{aligned} \text{Choice } B' \\ M_2 = 6.0 \times 10^{14} \text{ GeV} \\ M_3 = 6.1 \times 10^{14} \text{ GeV} \end{aligned} \quad (4.14)$$

which rephrase Eq.(3.19) and Eq.(3.22). The M_1 is proportional to r^2 with fixed m_4 given in Eq.(3.23).

Thermal leptogenesis can be explained without considering the flavor effect, if the process take above $T \sim 10^{12}$ GeV [42][43]. The sufficiently low value of M_1 relative to M_2 and M_3 implies that the asymmetry generated from the decays of N_2 and N_3 should have been washed out by subsequent inverse processes, and so only the ϵ_1 effectively contributed to the lepton asymmetry. In the case, $M_2 \gtrsim 3M_1$, only M_1 can contribute to Y_B , avoiding the resonant effect [38]. Thus, the r in Eq.(4.12) should have a lower bound about 0.21 to avoid the flavor consideration and an upper bound about 5.1 not to consider resonant models. Figure 2 shows the baryon asymmetry obtained upon the value of r in our choices.

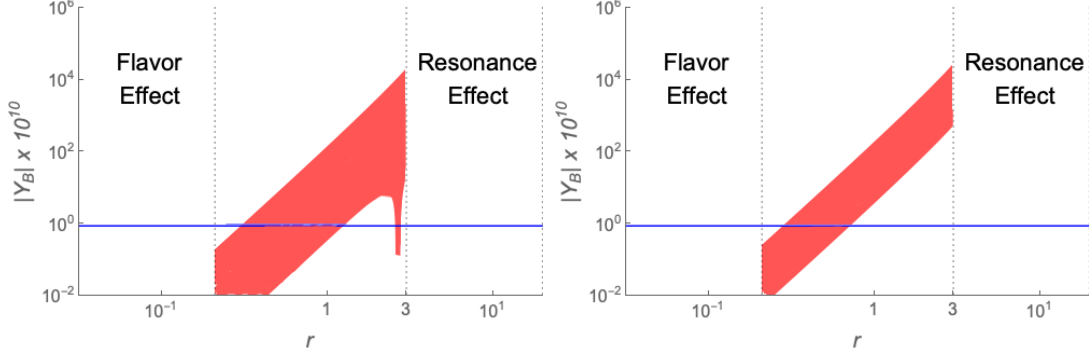


Figure 2. Baryon asymmetry's dependency on r for fixed Dirac phase, $\delta = 1.08\pi$ for NO(left) and $\delta = 1.58\pi$ for IO(right). Other Dirac phases and Majorana phases run in full ranges. The size of r has the direct correlation with M_1 in Eq.(4.12), and the vanilla leptogenesis model with our choices works for $0.21 < r < 2.95$. The blue line indicates the observed baryon asymmetry.

5 light sterile neutrino as probe of leptogenesis

The lepton asymmetry in both Choice A' and Choice B' is completely expressed in terms of elements of 4×4 unitary transformation for 3+1 light neutrinos. The survived asymmetry comes from mostly the decays of N_1 , and its size depends on the dilution factor and the CP asymmetry as $Y_L = \kappa_1 \epsilon_1 / g_*$. In $K_1 = K_1(\tilde{m}_1)$, the \tilde{m}_1 is determined by $(1 - |U_{s4}|^2)m_4/r^2$ using the mass relations in Eq.(3.19) and Eq.(3.22) and the $(\mathcal{Y}^\dagger \mathcal{Y})_{11}$ in Eq.(4.10) and Eq.(4.11). The CP asymmetry ϵ_1 is also expressed in terms of the mixing elements of sterile neutrino as in Eq.(4.10) and Eq.(4.11). The CP asymmetry cannot exist without the sterile neutrino and its mixing angles.

The only free parameter that affects the asymmetry is r , the dependence of which is shown in Fig.(2). For example, $r = 0.33$ is chosen to lead M_1 to the value 2.5×10^{12} GeV for the following estimation. According to the ranges in Eq.(3.23), the \tilde{m}_1 is allowed in $0.08 \sim 1.12$ eV, and thus the asymmetry took strong washout process because the possible range of K_1 run 74 to 1028 from the 3σ bounds. Hereafter, only best-fit values are adopted for the lepton asymmetry, because the uncertainties propagated from the 3σ ranges are exceeded by the ambiguities that arose from the additional Dirac phases δ_{24} and δ_{34} and Majorana phases η_1 , η_2 and η_3 .

5.1 m_{ee}

Although most phases in MES cannot be measured by current experiments, it is possible that m_{ee} measurements provide some bounds on the phases. At the end, the bounds could

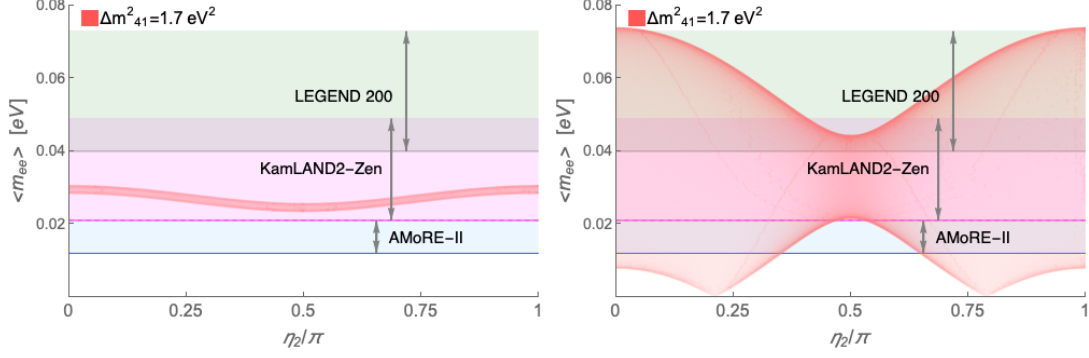


Figure 3. Effective electron-neutrino mass with 3+1 neutrinos m_{ee} versus a Majorana phase η_2 . (left) In NO case, running η_3 from 0 to π results in a relatively narrow band, while $m_1 = 0$. (right) In IO case, running η_1 from 0 to π results in a broad band, while $m_3 = 0$.

be tested by observed Y_B . For four neutrinos, m_{ee} is expressed,

$$\begin{aligned}
 |m'_{ee}|^2 = & m_1^2 |U'_{e1}|^4 + m_2^2 |U'_{e2}|^4 + m_3^2 |U'_{e3}|^4 + m_4^2 |U'_{e4}|^4 \\
 & + 2m_1 m_2 \cos 2(\eta_1 - \eta_2) |U'_{e1}|^2 |U'_{e2}|^2 \\
 & + 2m_1 m_3 \cos 2(\eta_1 - \eta_3 - \delta) |U'_{e1}|^2 |U'_{e3}|^2 \\
 & + 2m_1 m_4 \cos 2\eta_1 |U'_{e1}|^2 |U'_{e4}|^2 \\
 & + 2m_2 m_3 \cos 2(\eta_2 - \eta_3 - \delta) |U'_{e2}|^2 |U'_{e3}|^2 \\
 & + 2m_2 m_4 \cos 2\eta_2 |U'_{e2}|^2 |U'_{e4}|^2 \\
 & + 2m_3 m_4 \cos 2\eta_3 |U'_{e3}|^2 |U'_{e4}|^2,
 \end{aligned} \tag{5.1}$$

which reduces to $|m_{ee}|^2$ in Eq.(2.4) for three neutrinos.

Choice A' for NO: The zeroed m_1 removes the dependencies on η_1 in m'_{ee} , while it still keeps the dependencies of η_2 , η_3 , and δ . The application of the δ in 3σ range, 0.71 to 1.99 [58], to m'_{ee} does not cause a visual effect on the band in Fig.3(a), where the dominant contribution come from the last two terms of Eq.(5.1). So the figure simply shows the contribution only from both η_2 and η_3 variation 0 to π . There is a reference that showed the possibility to constrain m_4 and $\sin^2 2\theta_{14}$ using the close dependency between m_4 and m_{ee} for NO [64]. In comparison with the 3-neutrino m_{ee} in Fig.1, the 4-neutrino m_{ee} could be on the measurable range of KamLAND2-Zen and AMoRE II depending on the Δm_{41}^2 . Furthermore, the 3+1 model in NO with $\Delta m_{41}^2 \geq 1.7 \text{ eV}^2$ is not acceptable, if AMoRE II do not find $0\nu\beta\beta$ events.

Choice B' for IO: The zeroed m_3 removes the dependencies on η_3 and δ in m'_{ee} , while it still keeps the dependencies of η_1 and η_2 . The three dominant amplitudes in Eq.(5.1), $2m_1 m_2 |U'_{e1}|^2 |U'_{e2}|^2$, $2m_1 m_4 |U'_{e1}|^2 |U'_{e4}|^2$, and $2m_2 m_4 |U'_{e2}|^2 |U'_{e4}|^2$, contribute the shape of the broad band in Fig.3(b). It shows the strong sensitivity on both η_1 and η_2 . The three experiments mentioned in the above figures all have partial accessibility to find $0\nu\beta\beta$ events.

5.2 Y_B vs m_{ee}

In four-neutrino mixing matrix, there are two additional Dirac phases δ_{24} and δ_{34} , which cannot be determined by any known phenomenology either in low energy or in high energy. So the full range from 0 to π should be covered for both δ_{24} and δ_{34} . Furthermore, two Majorana phases should run almost full range until future neutrinoless double-beta decay experiments provide either positive or negative results in to reach the significant sensibility. We may seek for an indirect way in which the observation of the baryon asymmetry and the measurement of m_{ee} can constrain a combination of ranges in δ_{24} and δ_{34} as well as Majorana phases.

Choice A' for NO: Sufficient asymmetry in leptogenesis is obtained from the structure of \mathcal{Y}'_A and the ratios of M_1 to the others. The observation of the baryon asymmetry and the discovery of neutrinoless double-beta decay can constrain the CP phases, either Dirac or Majorana. However, it is unlikely that the combined constraints significantly narrow down the ranges in δ_{24} and δ_{34} , as well as those in η_2 and η_3 . In Fig 4, 9 cases are classified by combinations of δ_{24} and δ_{34} , setting 0, $\pi/2$ and π for each. As shown in the figure, a few combinations do not generate the asymmetry so as to reach the observation. The 3σ ranges in $|U_{\alpha 4}|^2$ in Eq.(3.23) do not make significant changes in Y_B , of which effects are undercover due to sweeping of η_2 and η_3 . Fig. 5 shows Y_B and m_{ee} in space of η_2 and η_3 for given values of $(\delta_{24}, \delta_{34})$. As $0\nu\beta\beta$ experiments improve their sensitivity, the exclusion region in η_2 and η_3 gets larger. More combinations of deltas can be rejected. For example, Fig.4 first rules out the combinations of $(\delta_{24}, \delta_{34})$, $(0, \frac{\pi}{2})$, $(0, \pi)$, $(\frac{\pi}{2}, 0)$, and $(\pi, 0)$ by Y_B^{obs} , and then Fig.5 rules out $(0, 0)$ and $(\frac{\pi}{2}, \pi)$ by $m_{ee} = 24$ meV. Only the orange area in Fig.5 is matched to Fig.4.

Choice B' for IO: Although M_2 and M_3 are almost degenerate, M_1 is low enough to produce the asymmetry effectively by itself and high enough to avoid the lepton flavor effect. Choice B' also has the ambiguity issue from untouchable phases δ_{24} and δ_{34} as well as η_1 and η_2 , as in Choice A' . Fig.6 includes 9 cases classified by combinations of δ_{24} and δ_{34} , setting 0, $\pi/2$ and π for each, and so does Fig. 7. Only the orange area in Fig.7 is matched to Fig.6 as in Choice A' . Fig.6 includes a few cases where m_{ee} has a range that is not compatible with Y_B^{obs} . When $(\delta_{24}, \delta_{34})$ is $(\pi, 0)$ or $(\pi, \frac{\pi}{2})$, for instance, there is no intersection between $m_{ee} = 30$ meV and Y_B^{obs} in positive area of Fig. 7. As a result, those combinations are ruled out.

6 Concluding remarks

We studied neutrino mass models in which three right-hand neutrinos steer the seesaw mechanism and their decays via Yukawa couplings produce the CP asymmetry from the interference between the tree level and one-loop levels. Accordingly the observed baryon asymmetry is explained such that it is converted from the lepton asymmetry by sphaleron process. The right-hand neutrinos couple with an additional light sterile neutrino besides the Yukawa couplings with active neutrinos, and so four light masses are leveraged by heavy neutrinos through the seesaw mechanism. The model is facilitated by choosing a real orthogonal transformations in Casas-Ibarra representation of seesaw mechanism. The real

transformation is given by a 4×3 matrix \mathcal{O}' that satisfies $\mathcal{O}'^T \mathcal{O}' = \mathbb{I}_{3 \times 3}$ but $\mathcal{O}' \mathcal{O}'^T \neq \mathbb{I}_{4 \times 4}$. It has been shown that specific $\mathcal{O}'_{\mathcal{A}}$ in Eq.(3.18) and $\mathcal{O}'_{\mathcal{B}}$ in Eq.(3.21) derives certain zero masses, for instance, $m_1 = 0$ for NO and $m_3 = 0$ for IO, respectively.

It is clear that the CP asymmetry cannot be obtained if the Yukawa matrix is factorized into the unitary mixing matrix U_ν and a real orthogonal matrix \mathcal{O} as in Eq.(3.4). However, if the Yukawa matrix depends on only the non-unitary partial block of a unitary 4×4 matrix U'_F in Eq.(3.16), then the CP asymmetry can be produced. Thus, the existence of the new Majorana field S and its couplings with Majorana neutrinos pushed up the Yukawa matrix to contribute to the lepton asymmetry Y_L . The MES for four neutrinos also can be derived with only two right-hand neutrinos as in minimal seesaw models. However, the resulting light masses consist of at least two zero masses that is not acceptable in phenomenology.

Two models dictated by \mathcal{O}'_A and \mathcal{O}'_B construct the masses in NO and IO, respectively. The observed Y_B^{obs} and the sensitivity of m_{ee} in near future have been taken to test the models. Four-neutrino global analysis provided the limits of $|U_{e4}|$, $|U_{\mu 4}|$, $|U_{\tau 4}|$ and $|U_{s4}|$ and there are various efforts in process to determine them. However, the improvement in precision of masses and mixing angles is eclipsed by the effect of a number of phases in four-neutrino theory. A series of figures, Fig.4 to Fig.7, show that the vagueness from additional phases, either Dirac or Majorana, looks difficult to clear out. The feature of our choice is that high energy legacy Y_B^{obs} can be explained by low energy measurable quantities, such as masses, mixing angles and phases of four neutrinos. Still there is one free parameter r we need to choose. It is possible to find excluded ranges in δ_{24} and δ_{34} when Y_B and m_{ee} are inspected simultaneously.

A 4×4 unitary transformation

The standard parametrization of 3×3 transformation matrix for three neutrinos can be expressed such as

$$V = R(\theta_{23}) R(\theta_{13}, \delta_{13}) R(\theta_{12}) = \begin{pmatrix} c_{12}c_{13} & s_{12}c_{13} & s_{13}e^{-i\delta} \\ -s_{12}c_{23} - c_{12}s_{23}s_{13}e^{i\delta} & c_{12}c_{23} - s_{12}s_{23}s_{13}e^{i\delta} & s_{23}c_{13} \\ s_{12}s_{23} - c_{12}c_{23}s_{13}e^{i\delta} & -c_{12}s_{23} - s_{12}c_{23}s_{13}e^{i\delta} & c_{23}c_{13} \end{pmatrix} \quad (\text{A.1})$$

where s_{ij} and c_{ij} denotes $\sin \theta_{ij}$ and $\cos \theta_{ij}$. For Majorana neutrinos, the transformation U is given by the product of V and P_2 , where

$$P_2 = \begin{pmatrix} e^{i\eta_1} & 0 & 0 \\ 0 & e^{i\eta_2} & 0 \\ 0 & 0 & 1 \end{pmatrix}. \quad (\text{A.2})$$

The matrix V is called U_{PMNS} and its elements are denoted as

$$U_{\text{PMNS}} = \begin{pmatrix} U_{e1} & U_{e2} & U_{e3} \\ U_{\mu 1} & U_{\mu 2} & U_{\mu 3} \\ U_{\tau 1} & U_{\tau 2} & U_{\tau 3} \end{pmatrix}. \quad (\text{A.3})$$

When a sterile neutrino with $T_{3L} = 0$ is added to the neutrino contents, the 4×4 unitary transformation can be denoted by

$$U'_F = \begin{pmatrix} U'_{e1} & U'_{e2} & U'_{e3} & U'_{e4} \\ U'_{\mu1} & U'_{\mu2} & U'_{\mu3} & U'_{\mu4} \\ U'_{\tau1} & U'_{\tau2} & U'_{\tau3} & U'_{\tau4} \\ U'_{s1} & U'_{s2} & U'_{s3} & U'_{s4} \end{pmatrix}, \quad (\text{A.4})$$

which consists of six rotations such as

$$U'_F = R(\theta_{34}, \delta_{34}) R(\theta_{24}, \delta_{24}) R(\theta_{14}) \begin{pmatrix} V & 0 \\ 0 & 1 \end{pmatrix} \quad (\text{A.5})$$

where each $R(\theta_{ij})$ is a 4×4 rotation matrix and the V is defined in Eq.(A.1). The elements of U'_F are specified in terms of mixing angles and phases of the sterile neutrino:

$$\begin{aligned} \begin{pmatrix} U'_{e1} \\ U'_{\mu1} \\ U'_{\tau1} \\ U'_{s1} \end{pmatrix} &= \begin{pmatrix} V_{11}c_{14} \\ -V_{11}s_{14}s_{24}e^{-i\delta_{24}} + V_{21}c_{24} \\ -V_{11}s_{14}s_{34}c_{24}e^{-i\delta_{34}} - V_{21}s_{24}s_{34}e^{i(\delta_{24}-\delta_{34})} + V_{31}c_{34} \\ -V_{11}s_{14}c_{24}c_{34} - V_{21}s_{24}c_{34}e^{i\delta_{24}} - V_{31}s_{34}e^{i\delta_{34}} \end{pmatrix} \\ \begin{pmatrix} U'_{e2} \\ U'_{\mu2} \\ U'_{\tau2} \\ U'_{s2} \end{pmatrix} &= \begin{pmatrix} V_{12}c_{14} \\ -V_{12}s_{14}s_{24}e^{-i\delta_{24}} + V_{22}c_{24} \\ -V_{12}s_{14}s_{34}c_{24}e^{-i\delta_{34}} - V_{22}s_{24}s_{34}e^{i(\delta_{24}-\delta_{34})} + V_{32}c_{34} \\ -V_{12}s_{14}c_{24}c_{34} - V_{22}s_{24}c_{34}e^{-i\delta_{24}} - V_{32}s_{34}e^{i\delta_{34}} \end{pmatrix} \\ \begin{pmatrix} U'_{e3} \\ U'_{\mu3} \\ U'_{\tau3} \\ U'_{s3} \end{pmatrix} &= \begin{pmatrix} V_{13}c_{14} \\ -V_{13}s_{14}s_{24} + V_{23}c_{24}e^{-i\delta_{24}} \\ -V_{13}s_{14}s_{34}c_{24}e^{-i\delta_{34}} - V_{23}s_{24}s_{34}e^{i(\delta_{24}-\delta_{34})} + V_{33}c_{34} \\ -V_{13}s_{14}c_{24}c_{34} - V_{23}s_{24}c_{34}e^{i\delta_{24}} - V_{33}s_{34}e^{i\delta_{34}} \end{pmatrix} \\ \begin{pmatrix} U'_{e4} \\ U'_{\mu4} \\ U'_{\tau4} \\ U'_{s4} \end{pmatrix} &= \begin{pmatrix} s_{14} \\ s_{24}c_{14}e^{-i\delta_{24}} \\ s_{34}c_{14}c_{24}e^{-i\delta_{34}} \\ c_{14}c_{24}c_{34} \end{pmatrix} \end{aligned} \quad (\text{A.6})$$

For the transformation of Majorana neutrinos, the diagonal phase transformation with three Majorana phases also here is attached such that $U' = U'_F P_3$ with the following diagonal phase transformation:

$$P_3 = \begin{pmatrix} e^{i\eta_1} & 0 & 0 & 0 \\ 0 & e^{i\eta_2} & 0 & 0 \\ 0 & 0 & e^{i\eta_3} & 0 \\ 0 & 0 & 0 & 1 \end{pmatrix}. \quad (\text{A.7})$$

The individual rotation angle can be expressed in terms of the elements of U'_F ,

$$\begin{aligned} s_{14}^2 &= |U'_{e4}|^2 \\ s_{24}^2 &= |U'_{\mu4}|^2(1 - |U'_{e4}|^2)^{-1} \\ s_{34}^2 &= |U'_{\tau4}|^2(1 - |U'_{e4}|^2 - |U'_{\mu4}|^2)^{-1} \end{aligned} \quad (\text{A.8})$$

where $|U'_{s4}|^2 = 1 - |U'_{e4}|^2 - |U'_{\mu4}|^2 - |U'_{\tau4}|^2$.

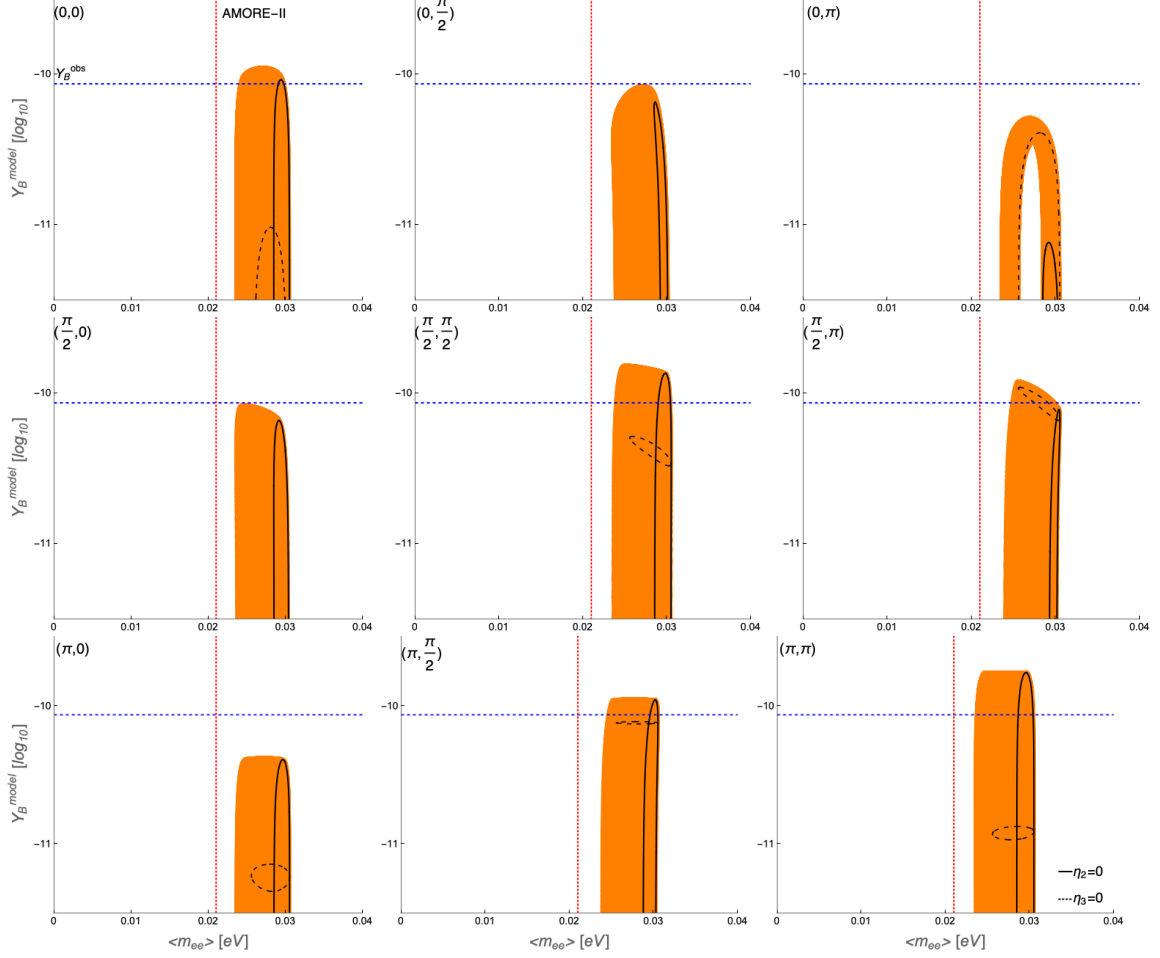


Figure 4. Y_B vs. m_{ee} for given choice of $(\delta_{24}, \delta_{34})$ in Choice A' . Majorana phases η_2 and η_3 run fully 0 to π so as to cover the colored area. The blue dotted horizontal line at $(8.61 \pm 0.05) \times 10^{-11}$ indicates the observed baryon asymmetry, while the red dotted vertical line at 21 meV indicates the upper bound of sensitivity of AMoRE II. The solid and dashed lines inside each shade mark the criteria, $\eta_2 = 0$ and $\eta_3 = 0$, respectively. Only positive results are presented.

Acknowledgments

This work was supported by NRF grant funded by MSIT of Korea (NRF-2022R1A2C1009686) and by the Chung-Ang University research grant in 2019.

References

- [1] **DUNE** Collaboration, B. Abi et al., *Deep Underground Neutrino Experiment (DUNE), Far Detector Technical Design Report, Volume I Introduction to DUNE*, **JINST** **15** (2020), no. 08 T08008, [[arXiv:2002.02967](#)].
- [2] **Hyper-Kamiokande** Collaboration, K. Abe et al., *Hyper-Kamiokande Design Report*, [arXiv:1805.04163](#).

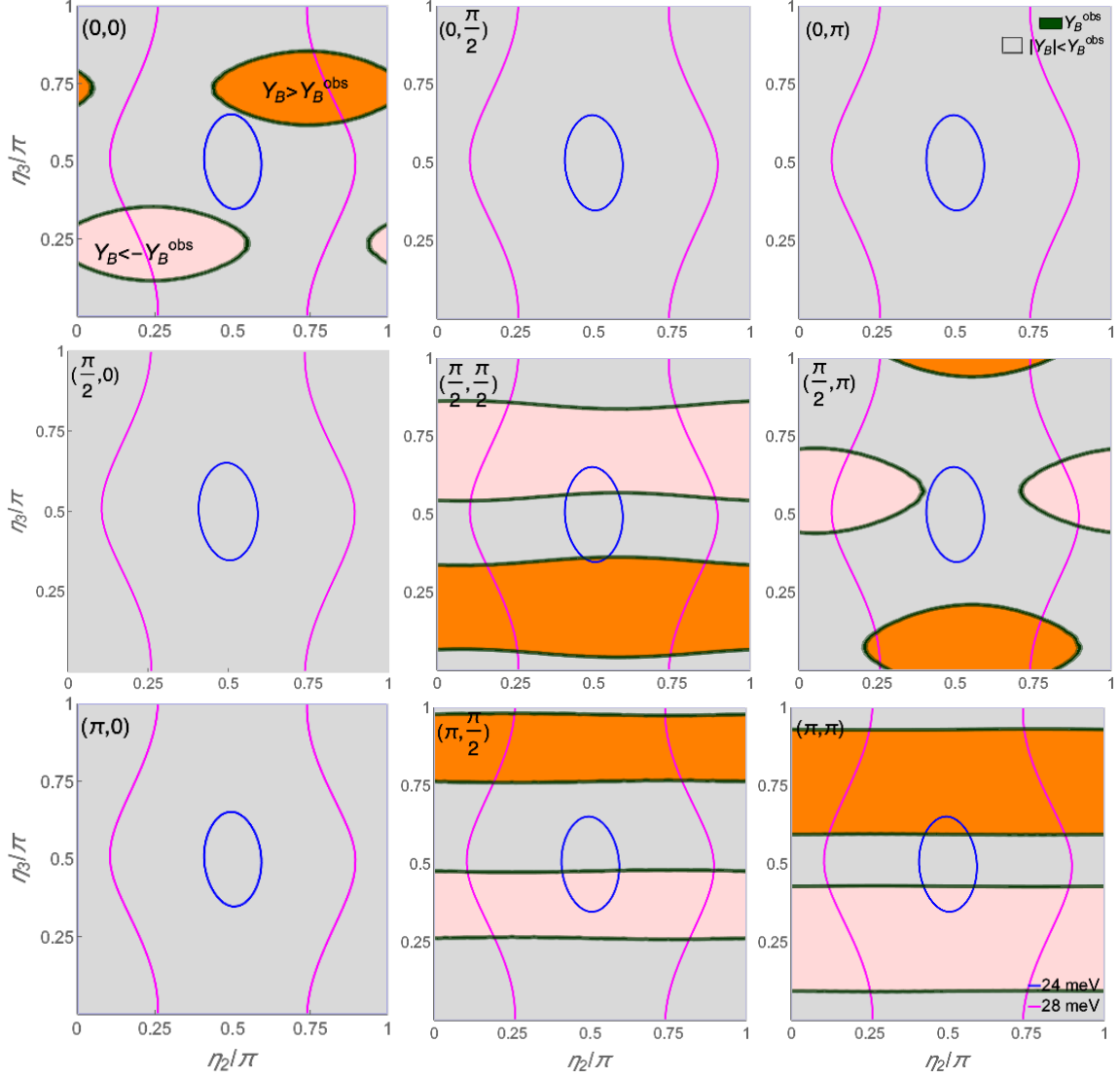


Figure 5. Contours of Y_B and m_{ee} in $\eta_3 - \eta_2$ space for given choice of $(\delta_{24}, \delta_{34})$ in Choice A' . The contour of $m_{ee} = 28$ meV (24 meV) is represented by magenta (blue) solid line. The green curves Y_B^{obs} correspond to the contours matched to the observation. The gray areas represent $|Y_B| < Y_B^{\text{obs}}$, while the orange and pink areas represent $Y_B > Y_B^{\text{obs}}$ and $Y_B < -Y_B^{\text{obs}}$, respectively.

- [3] B. Pontecorvo, *Neutrino Experiments and the Problem of Conservation of Leptonic Charge*, Zh. Eksp. Teor. Fiz. **53** (1967) 1717–1725.
- [4] Z. Maki, M. Nakagawa, and S. Sakata, *Remarks on the unified model of elementary particles*, Prog. Theor. Phys. **28** (1962) 870–880.
- [5] M. Agostini, G. Benato, and J. Detwiler, *Discovery probability of next-generation neutrinoless double- β decay experiments*, Phys. Rev. D **96** (2017), no. 5 053001, [[arXiv:1705.02996](#)].
- [6] **CUORE** Collaboration, C. Alduino et al., *First Results from CUORE: A Search for Lepton Number Violation via $0\nu\beta\beta$ Decay of ^{130}Te* , Phys. Rev. Lett. **120** (2018), no. 13 132501, [[arXiv:1710.07988](#)].

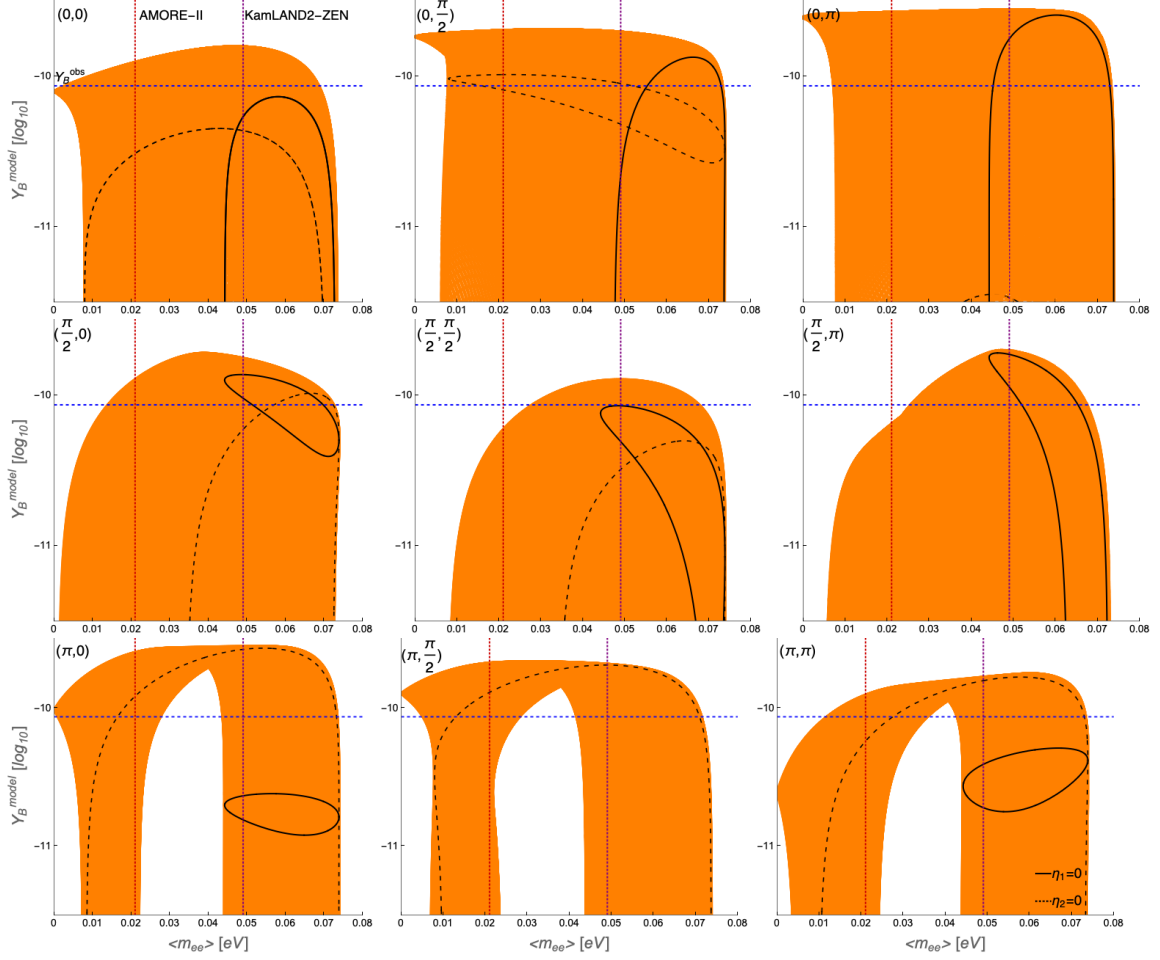


Figure 6. Y_B vs. m_{ee} for given choice of $(\delta_{24}, \delta_{34})$ in Choice B' . Majorana phases η_1 and η_2 run fully 0 to π so as to cover the colored area. The horizontal dotted blue line at $(8.61 \pm 0.05) \times 10^{-11}$ indicates the observed baryon asymmetry, while the vertical two lines at 21 meV and 49 meV indicate the upper bounds of sensitivities of AMORE II and KamLAND2-Zen, respectively. The solid and dashed lines inside each shade mark the criteria $\eta_1 = 0$ and $\eta_2 = 0$, respectively. Only positive results are presented.

- [7] **GERDA** Collaboration, M. Agostini et al., *Improved Limit on Neutrinoless Double- β Decay of ^{76}Ge from GERDA Phase II*, Phys. Rev. Lett. **120** (2018), no. 13 132503, [[arXiv:1803.11100](#)].
- [8] **Majorana** Collaboration, C. E. Aalseth et al., *Search for Neutrinoless Double- β Decay in ^{76}Ge with the Majorana Demonstrator*, Phys. Rev. Lett. **120** (2018), no. 13 132502, [[arXiv:1710.11608](#)].
- [9] **EXO-200** Collaboration, J. B. Albert et al., *Search for nucleon decays with EXO-200*, Phys. Rev. D **97** (2018), no. 7 072007, [[arXiv:1710.07670](#)].
- [10] **CUPID-0** Collaboration, O. Azzolini et al., *First Result on the Neutrinoless Double- β Decay of ^{82}Se with CUPID-0*, Phys. Rev. Lett. **120** (2018), no. 23 232502, [[arXiv:1802.07791](#)].
- [11] **SNO+** Collaboration, V. Fischer, *Search for neutrinoless double-beta decay with SNO+*, in

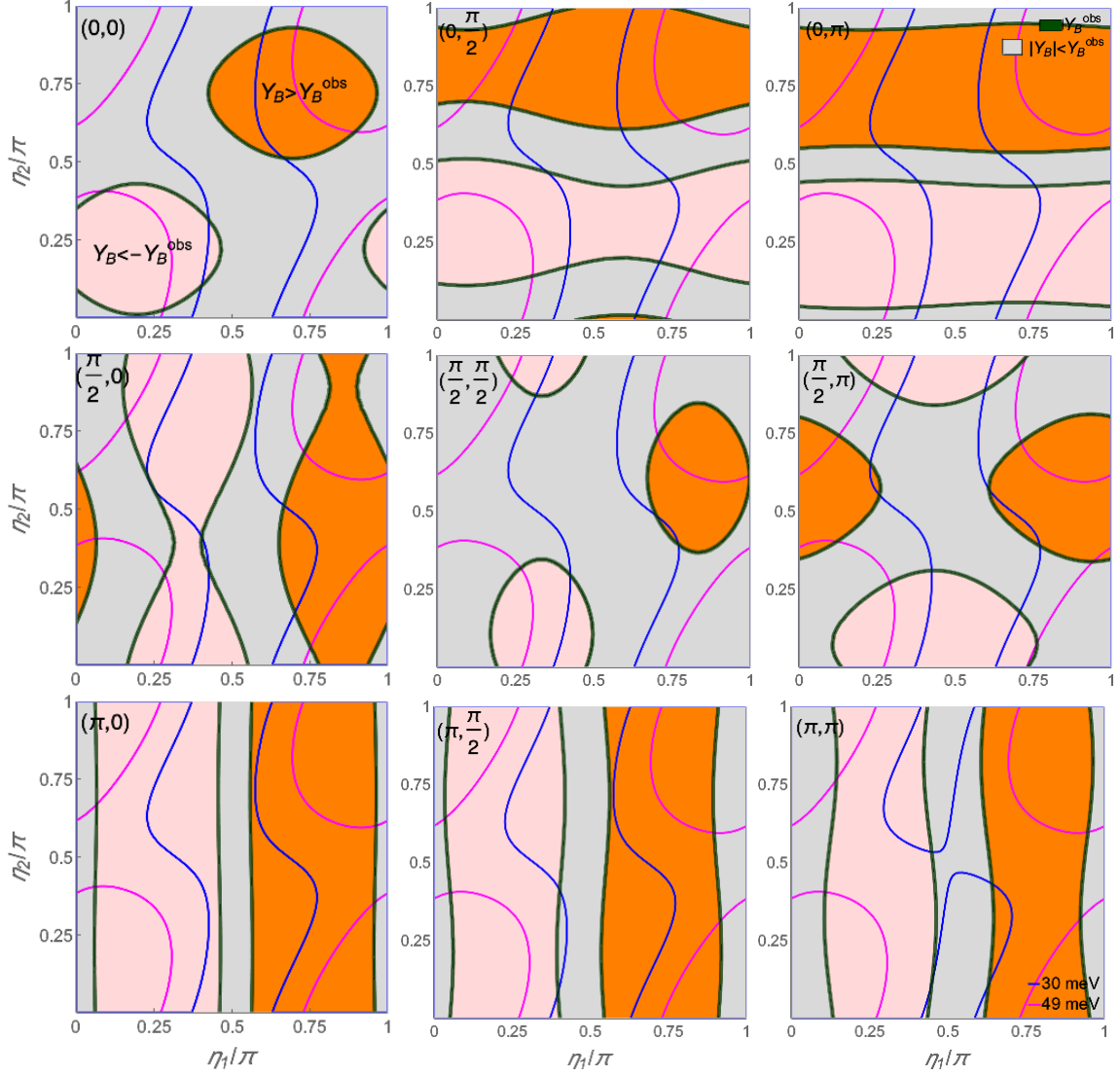


Figure 7. Contours of Y_B and m_{ee} in $\eta_2 - \eta_1$ space for given choice of $(\delta_{24}, \delta_{34})$ in Choice B' . The contour of $m_{ee} = 49$ meV (30 meV) is represented by magenta (blue) line. The green curves Y_B^{obs} correspond to the contours matched to the observation. The gray areas represent $|Y_B| < Y_B^{\text{obs}}$, while the orange and pink areas represent $Y_B > Y_B^{\text{obs}}$ and $Y_B < -Y_B^{\text{obs}}$, respectively.

13th Conference on the Intersections of Particle and Nuclear Physics, 9, 2018.

[arXiv:1809.05986](https://arxiv.org/abs/1809.05986).

- [12] **NEXT** Collaboration, J. Martín-Albo et al., *Sensitivity of NEXT-100 to Neutrinoless Double Beta Decay*, *JHEP* **05** (2016) 159, [[arXiv:1511.09246](https://arxiv.org/abs/1511.09246)].
- [13] V. Alenkov et al., *First Results from the AMoRE-Pilot neutrinoless double beta decay experiment*, *Eur. Phys. J. C* **79** (2019), no. 9 791, [[arXiv:1903.09483](https://arxiv.org/abs/1903.09483)].
- [14] A. S. Barabash et al., *Calorimeter development for the SuperNEMO double beta decay experiment*, *Nucl. Instrum. Meth. A* **868** (2017) 98–108, [[arXiv:1707.06823](https://arxiv.org/abs/1707.06823)].
- [15] **LEGEND** Collaboration, N. Abgrall et al., *The Large Enriched Germanium Experiment for*

- Neutrinoless Double Beta Decay (LEGEND)*, *AIP Conf. Proc.* **1894** (2017), no. 1 020027, [[arXiv:1709.01980](#)].
- [16] **KamLAND-Zen** Collaboration, A. Gando et al., *Search for Majorana Neutrinos near the Inverted Mass Hierarchy Region with KamLAND-Zen*, *Phys. Rev. Lett.* **117** (2016), no. 8 082503, [[arXiv:1605.02889](#)]. [Addendum: *Phys. Rev. Lett.* **117**, 109903 (2016)].
 - [17] **AMoRE** Collaboration, V. Alenkov et al., *Technical Design Report for the AMoRE $0\nu\beta\beta$ Decay Search Experiment*, [[arXiv:1512.05957](#)].
 - [18] **NEOS** Collaboration, Y. J. Ko et al., *Sterile Neutrino Search at the NEOS Experiment*, *Phys. Rev. Lett.* **118** (2017), no. 12 121802, [[arXiv:1610.05134](#)].
 - [19] **PROSPECT** Collaboration, J. Ashenfelter et al., *First search for short-baseline neutrino oscillations at HFIR with PROSPECT*, *Phys. Rev. Lett.* **121** (2018), no. 25 251802, [[arXiv:1806.02784](#)].
 - [20] **DANSS** Collaboration, I. Alekseev et al., *Search for sterile neutrinos at the DANSS experiment*, *Phys. Lett. B* **787** (2018) 56–63, [[arXiv:1804.04046](#)].
 - [21] A. P. Serebrov et al., *Search for sterile neutrinos with the Neutrino-4 experiment and measurement results*, *Phys. Rev. D* **104** (2021), no. 3 032003, [[arXiv:2005.05301](#)].
 - [22] **SoLid** Collaboration, Y. Abreu et al., *SoLid: a short baseline reactor neutrino experiment*, *JINST* **16** (2021), no. 02 P02025, [[arXiv:2002.05914](#)].
 - [23] **STEREO** Collaboration, H. Almazán et al., *Sterile Neutrino Constraints from the STEREO Experiment with 66 Days of Reactor-On Data*, *Phys. Rev. Lett.* **121** (2018), no. 16 161801, [[arXiv:1806.02096](#)].
 - [24] **RENO, NEOS** Collaboration, Z. Atif et al., *Search for sterile neutrino oscillation using RENO and NEOS data*, [[arXiv:2011.00896](#)].
 - [25] **LSND** Collaboration, A. Aguilar-Arevalo et al., *Evidence for neutrino oscillations from the observation of $\bar{\nu}_e$ appearance in a $\bar{\nu}_\mu$ beam*, *Phys. Rev. D* **64** (2001) 112007, [[hep-ex/0104049](#)].
 - [26] **MiniBooNE** Collaboration, A. A. Aguilar-Arevalo et al., *Significant Excess of ElectronLike Events in the MiniBooNE Short-Baseline Neutrino Experiment*, *Phys. Rev. Lett.* **121** (2018), no. 22 221801, [[arXiv:1805.12028](#)].
 - [27] P. A. Machado, O. Palamara, and D. W. Schmitz, *The Short-Baseline Neutrino Program at Fermilab*, *Ann. Rev. Nucl. Part. Sci.* **69** (2019) 363–387, [[arXiv:1903.04608](#)].
 - [28] S. Ajimura et al., *Proposal: JSNS²-II*, [[arXiv:2012.10807](#)].
 - [29] V. A. Kuzmin, V. A. Rubakov, and M. E. Shaposhnikov, *On the Anomalous Electroweak Baryon Number Nonconservation in the Early Universe*, *Phys. Lett. B* **155** (1985) 36.
 - [30] M. Fukugita and T. Yanagida, *Baryogenesis Without Grand Unification*, *Phys. Lett. B* **174** (1986) 45–47.
 - [31] M. A. Luty, *Baryogenesis via leptogenesis*, *Phys. Rev. D* **45** (1992) 455–465.
 - [32] **Planck** Collaboration, N. Aghanim et al., *Planck 2018 results. I. Overview and the cosmological legacy of Planck*, *Astron. Astrophys.* **641** (2020) A1, [[arXiv:1807.06205](#)].
 - [33] A. D. Sakharov, *Violation of CP Invariance, C asymmetry, and baryon asymmetry of the universe*, *Pisma Zh. Eksp. Teor. Fiz.* **5** (1967) 32–35.

- [34] J. A. Harvey and M. S. Turner, *Cosmological baryon and lepton number in the presence of electroweak fermion number violation*, Phys. Rev. D **42** (1990) 3344–3349.
- [35] L. Covi, E. Roulet, and F. Vissani, *CP violating decays in leptogenesis scenarios*, Phys. Lett. B **384** (1996) 169–174, [[hep-ph/9605319](#)].
- [36] E. Roulet, L. Covi, and F. Vissani, *On the CP asymmetries in Majorana neutrino decays*, Phys. Lett. B **424** (1998) 101–105, [[hep-ph/9712468](#)].
- [37] H. B. Nielsen and Y. Takahashi, *Baryogenesis via lepton number violation in anti-GUT model*, Phys. Lett. B **507** (2001) 241–251, [[hep-ph/0101307](#)].
- [38] Z.-z. Xing and Z.-h. Zhao, *The minimal seesaw and leptogenesis models*, Rept. Prog. Phys. **84** (2021), no. 6 066201, [[arXiv:2008.12090](#)].
- [39] S. K. Kang, *Low-energy CP violation and leptogenesis in a minimal seesaw model*, J. Korean Phys. Soc. **78** (2021), no. 9 743–749.
- [40] S. Chang, S. K. Kang, and K. Siyeon, *Minimal seesaw model with tri/bi-maximal mixing and leptogenesis*, Phys. Lett. B **597** (2004) 78–88, [[hep-ph/0404187](#)].
- [41] K. Siyeon, *Seesaw Scale and CP Phases in a Minimal Model of Leptogenesis*, J. Korean Phys. Soc. **69** (2016), no. 11 1638–1643, [[arXiv:1611.04572](#)].
- [42] A. Abada, S. Davidson, A. Ibarra, F. X. Josse-Michaux, M. Losada, and A. Riotto, *Flavour Matters in Leptogenesis*, JHEP **09** (2006) 010, [[hep-ph/0605281](#)].
- [43] E. Nardi, Y. Nir, E. Roulet, and J. Racker, *The Importance of flavor in leptogenesis*, JHEP **01** (2006) 164, [[hep-ph/0601084](#)].
- [44] K. Moffat, S. Pascoli, S. T. Petcov, and J. Turner, *Leptogenesis from Low Energy CP Violation*, JHEP **03** (2019) 034, [[arXiv:1809.08251](#)].
- [45] A. Pilaftsis and T. E. J. Underwood, *Resonant leptogenesis*, Nucl. Phys. B **692** (2004) 303–345, [[hep-ph/0309342](#)].
- [46] J. A. Casas and A. Ibarra, *Oscillating neutrinos and $\mu \rightarrow e, \gamma$* , Nucl. Phys. B **618** (2001) 171–204, [[hep-ph/0103065](#)].
- [47] W. Rodejohann, *On Non-Unitary Lepton Mixing and Neutrino Mass Observables*, Phys. Lett. B **684** (2010) 40–47, [[arXiv:0912.3388](#)].
- [48] J. Barry, W. Rodejohann, and H. Zhang, *Light Sterile Neutrinos: Models and Phenomenology*, JHEP **07** (2011) 091, [[arXiv:1105.3911](#)].
- [49] H. Zhang, *Light Sterile Neutrino in the Minimal Extended Seesaw*, Phys. Lett. B **714** (2012) 262–266, [[arXiv:1110.6838](#)].
- [50] N. Nath, M. Ghosh, S. Goswami, and S. Gupta, *Phenomenological study of extended seesaw model for light sterile neutrino*, JHEP **03** (2017) 075, [[arXiv:1610.09090](#)].
- [51] S. Goswami, V. K. N., A. Mukherjee, and N. Narendra, *Leptogenesis and eV scale sterile neutrino*, Phys. Rev. D **105** (2022), no. 9 095040, [[arXiv:2111.14719](#)].
- [52] C. Giunti and E. M. Zavanin, *Predictions for Neutrinoless Double-Beta Decay in the 3+1 Sterile Neutrino Scenario*, JHEP **07** (2015) 171, [[arXiv:1505.00978](#)].
- [53] S. Parke and M. Ross-Lonergan, *Unitarity and the three flavor neutrino mixing matrix*, Phys. Rev. D **93** (2016), no. 11 113009, [[arXiv:1508.05095](#)].

- [54] S. Gariazzo, C. Giunti, M. Laveder, and Y. F. Li, *Updated Global 3+1 Analysis of Short-BaseLine Neutrino Oscillations*, JHEP **06** (2017) 135, [[arXiv:1703.00860](#)].
- [55] **T2K** Collaboration, K. Abe et al., *Constraint on the matter–antimatter symmetry-violating phase in neutrino oscillations*, Nature **580** (2020), no. 7803 339–344, [[arXiv:1910.03887](#)]. [Erratum: Nature 583, E16 (2020)].
- [56] **NOvA** Collaboration, M. A. Acero et al., *First Measurement of Neutrino Oscillation Parameters using Neutrinos and Antineutrinos by NOvA*, Phys. Rev. Lett. **123** (2019), no. 15 151803, [[arXiv:1906.04907](#)].
- [57] **Particle Data Group** Collaboration, P. A. Zyla et al., *Review of Particle Physics*, PTEP **2020** (2020), no. 8 083C01.
- [58] P. F. de Salas, D. V. Forero, S. Gariazzo, P. Martínez-Miravé, O. Mena, C. A. Ternes, M. Tórtola, and J. W. F. Valle, *2020 global reassessment of the neutrino oscillation picture*, JHEP **02** (2021) 071, [[arXiv:2006.11237](#)].
- [59] I. Esteban, M. C. Gonzalez-Garcia, M. Maltoni, T. Schwetz, and A. Zhou, *The fate of hints: updated global analysis of three-flavor neutrino oscillations*, JHEP **09** (2020) 178, [[arXiv:2007.14792](#)].
- [60] **ATLAS** Collaboration, G. Aad et al., *Observation of a new particle in the search for the Standard Model Higgs boson with the ATLAS detector at the LHC*, Phys. Lett. B **716** (2012) 1–29, [[arXiv:1207.7214](#)].
- [61] **CMS** Collaboration, S. Chatrchyan et al., *Observation of a New Boson at a Mass of 125 GeV with the CMS Experiment at the LHC*, Phys. Lett. B **716** (2012) 30–61, [[arXiv:1207.7235](#)].
- [62] A. Pilaftsis, *Heavy Majorana neutrinos and baryogenesis*, Int. J. Mod. Phys. A **14** (1999) 1811–1858, [[hep-ph/9812256](#)].
- [63] S. Davidson and A. Ibarra, *A Lower bound on the right-handed neutrino mass from leptogenesis*, Phys. Lett. B **535** (2002) 25–32, [[hep-ph/0202239](#)].
- [64] C. H. Jang, B. J. Kim, Y. J. Ko, and K. Siyeon, *Neutrinoless Double Beta Decay and Light Sterile Neutrino*, J. Korean Phys. Soc. **73** (2018), no. 11 1625–1630, [[arXiv:1811.09957](#)].